NREL
NATIONAL RENEWABLE ENERGY LABORATORY

Thickness Effect of Al-Doped ZnO Window Layer on Damp Heat Stability of CuInGaSe2 Solar Cells

Preprint

F.J. Pern, L. Mansfield, C. DeHart, S.H. Glick, F. Yan, and R. Noufi

Presented at the 37th IEEE Photovoltaic Specialists Conference (PVSC 37)
Seattle, Washington
June 19-24, 2011

Conference Paper
NREL/CP-5200-50682
July 2011

Contract No. DE-AC36-08GO28308

Available electronically at http://www.osti.gov/bridge

Available for a processing fee to U.S. Department of Energy
and its contractors, in paper, from:

U.S. Department of Energy
Office of Scientific and Technical Information

P.O. Box 62
Oak Ridge, TN 37831-0062
phone: 865.576.8401
fax: 865.576.5728
email: mailto:reports@adonis.osti.gov

Available for sale to the public, in paper, from:

U.S. Department of Commerce
National Technical Information Service
5285 Port Royal Road
Springfield, VA 22161
phone: 800.553.6847
fax: 703.605.6900
email: orders@ntis.fedworld.gov
online ordering: http://www.ntis.gov/help/ordermethods.aspx

Cover Photos: (left to right) PIX 16416, PIX 17423, PIX 16560, PIX 17613, PIX 17436, PIX 17721

Printed on paper containing at least 50% wastepaper, including 10% post consumer waste.

THICKNESS EFFECT OF Al-DOPED ZnO WINDOW LAYER ON DAMP-HEAT STABILITY OF $CuInGaSe_2$ SOLAR CELLS

F.J. Pern, L. Mansfield, C. DeHart, S.H. Glick, F. Yan, and R. Noufi
National Center for Photovoltaics, National Renewable Energy Laboratory, 1617 Cole Blvd., Golden, CO 80401, USA

ABSTRACT

We investigated the damp heat (DH) stability of $CuInGaSe_2$ (CIGS) solar cells as a function of thickness of the Al-doped ZnO (AZO) window layer from the "standard" 0.12 μm to a modest 0.50 μm over an underlying 0.10-μm intrinsic ZnO buffer layer. The CIGS cells were prepared with external electrical contact using fine Au wire to the tiny "standard" Ni/Al (0.05 μm/3 μm) metal grid contact pads. Bare cell coupons and sample sets encapsulated in a specially designed, Al-frame test structure with an opening for moisture ingress control using a TPT backsheet were exposed to DH at 85°C and 85% relative humidity, and characterized by current-voltage (I-V), quantum efficiency (QE), and (electrochemical) impedance spectroscopy (ECIS). The results show that bare cells exhibited rapid degradation within 50-100 h, accompanied by film wrinkling and delamination and corrosion of Mo and AlNi grid, regardless of AZO thickness. In contrast, the encapsulated cells did not show film wrinkling, delamination, and Mo corrosion after 168 h DH exposure; but the trend of efficiency degradation rate showed a weak correlation to the AZO thickness.

INTRODUCTION

Long-term performance reliability is critical for CIGS photovoltaic (PV) modules. The IEC 61646 qualification standard for terrestrial thin film modules requires a stringent DH test at 85°C and 85% relative humidity (RH) for 1000 h. A high percentage of thin-film modules reportedly failed in this test. The CIGS cell component materials, including Mo, CIGS, and ZnO, have been shown by us [1–4] and others to be DH sensitive or unstable. For improving the performance reliability of thin-film CIGS modules, several approaches can be employed to minimize the damaging impact of moisture ingress. Among them, use of desiccant-type edge sealant has been widely used for glass-glass module construction. Addition of a thin moisture barrier film to the encapsulation is being eagerly pursued for flexible CIGS modules. At NREL, we have investigated alternate approaches by using (i) a layer of DH-stable, transparent moisture barrier deposited directly on the CIGS solar cells, and (ii) a DH-stable TCO such as ITO or InZnO to replace the AZO window layer [5]. However the second method could increase the cost by greater use of expensive In metal. A much preferred approach is one that can preserve the high performance of the solar cell while not changing well-established fabrication process and causing significant cost increase. In a previous study on DH stability of various TCOs on glass substrates, we found that, as the AZO layer thickness increased from the "standard" 0.12 μm to 0.50 μm, its DH stability showed a large enhancement with little to no decrease in optical and electrical properties [1]. Although the exact mechanism for the improved DH stability has not been clear yet, we have engaged in an effort to apply thicker AZO layers to the CIGS solar cells without changing any fabrication process conditions and materials. Their DH stability is the main subject of this paper. We also developed the means for making DH-stable external electrical contacts and test structure for encapsulation to ensure that the observed DH instability is from the CIGS solar cell and its component materials, rather that from the contact degradation. We employed I-V, QE, ECIS, PL, and EL to characterize the solar cells. With the potential for *in-situ* monitoring, ECIS is being evaluated as a sensitive, non-invasive, non-destructive analytical method for the CIGS solar cells [6–12].

EXPERIMENTAL

Solar cells and AZO layers. The solar cells were prepared on 0.7-μm Mo-coated soda lime glass with 1.5–2 μm CIGS absorber by NREL's 3-stage thermal coevaporation process, followed by ~0.05-μm CBD CdS, 0.10-μm i-ZnO, and various thickness of AZO (0.12, 0.24, 0.36, and 0.50 μm) deposited in a Semicore RF sputtering system. The four AZO thicknesses required 8, 16, 25, and 35 passes, respectively, of the substrate holder platform moving over the sputtering target. The temperature monitored with temperature indicator strips (Omega, P/N 8MA) showed <65°C for 0.12-μm AZO, >77°C for 0.24 μm, >121°C for 0.36 μm, and >138°C for 0.50 μm, respectively.

External electrical contact. To avoid potential damage by repeated electrical measurements to the tiny AlNi square pads on the cells, external connection was made to the small contact pad on each device with a small dot of silver paste and a low-melting-point (m.p. 118°C or 143°C) solder alloy followed by attaching a 4.5-mil Au wire by soldering. Depending on test needs, the other end of the Au wire was soldered on tab ribbon pieces secured either on edge sealant tapes over a 7.6-cm x 7.6-cm (3" x 3") glass plate or outside the Al-frame test structure after being encapsulated. Au wire was also soldered to the In strip applied on the Mo surface of the cell coupon and a piece of tab ribbon.

Test Structure and Encapsulation. A specially designed and machined 10.16-cm x 10.16-cm x 6.35-mm (4" x 4" x ¼") Al plate with a 70-mm x 70-mm x 2.75-mm square cut-off "well" was used to secure cell samples. Encapsulation was made between a 3.2-mm thick borosilicate (borofloat)

glass plate on the top and a 10.16-cm x 10.16-cm x 1.6-mm Al back plate on the bottom with two layers of TruSeal's SET LP01 gray edge sealant tape (12.7 mm wide, 1.0 mm thick), creating a net chamber volume of ~220 mm^3 (~134 mm^3 without edge sealant tapes) when laminated empty at 100°C. Both the Al frame and plate had a 1.25-cm x 1.25-cm opening in the center for moisture ingress control by sandwiching a piece of multilayer film. Several films having different water vapor transmission rates (WVTR), measured on a Mocon Permatran-W 3/33 system at 100% RH, were chosen for moisture ingress control. This paper reports the results for the sample "Set 5" using Madico's primed TPT (Tedlar/polyester/Tedlar) backsheet.

Characterization. Transmission and reflection spectra were measured on a Cary 6000i spectrophotometer. I-V measurements were performed on an Optical Radiation Corp. model 1000 solar simulator, and QE on a custom-built system. ECIS used an SI 1260 impedance/gain-phase analyzer and an SI 1286 electrochemical interface from Schlumberger Technologies, operated with the ZPlot and ZView software from Scribner Associates. Before and after wire soldering and encapsulation, and periodically during DH exposure, the CIGS cell coupons were measured with I-V, QE, and ECIS in the dark. Some samples were imaged with photoluminescence (PL) and electroluminescence (EL).

RESULTS AND DISCUSSION

I. DH stability and optical properties of AZO films

We reported previously that the DH stability of AZO on glass increased as the film's thickness increased—the AZO films at ~0.5 μm showed essentially no decrease in optical and electrical properties after 778-h DH exposure, despite a small degree of morphological change on the film's surface feature as revealed by SEM micro-images [1]. The reason for this increased DH stability may be due to increased temperature during film deposition from <65°C for the standard 0.12 μm to >138°C for a 0.50 μm film. The result suggests that if applied on a CIGS solar cell, the cell's DH stability may be improved accordingly. Therefore, we prepared a series of samples of bilyer ZnO (BZO, i.e., AZO with the standard 0.10-μm i-ZnO underneath) on CIGS solar cells and glass substrates. The thicker BZO films on glass and CIGS solar cells produced stronger (002) peak intensity in XRD analysis (not shown), suggesting the presence of greater crystallinity from thickness and temperature effects. Their transmittance and reflectance spectra are shown in Fig. 1. As the AZO layer became thicker, there is some loss in T%, particularly in the 1050–1500-nm range due to ionized-carrier absorption. However, the net effect of optical loss due to increased AZO thickness on the BZO/CIGS solar cells is not so large, because the cells' spectral responses are primarily in the 400–1050 nm range as illustrated in Fig. 2, showing the QE spectra of some cells with four different AZO thicknesses. This is significant because it is possible to use even thicker AZO window layer without severe spectral loss for the CIGS cells, if the thicker AZO is proved to greatly enhance the cell's DH stability.

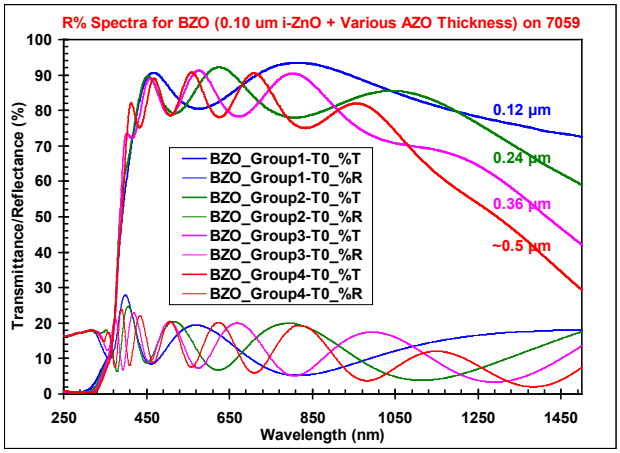

Figure 1 Transmittance and reflectance spectra as a function of bilayer ZnO (BZO) with different thickness Al-doped ZnO on 0.10 μm i-ZnO.

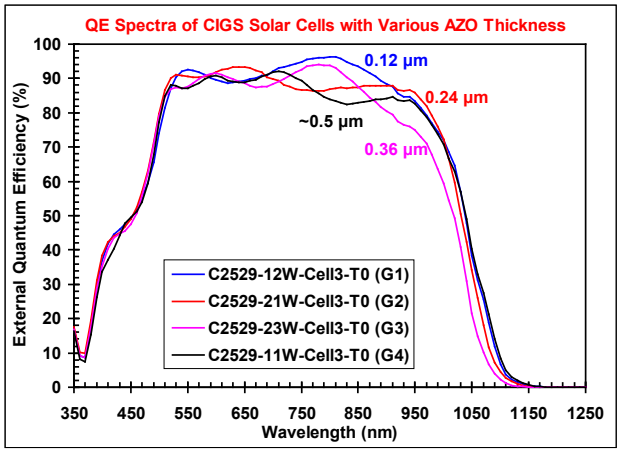

Figure 2 External quantum efficiency spectra measured for CIGS solar cells with BZO of different thickness Al-doped ZnO on 0.10 μm i-ZnO.

II. DH stability of bare cell coupons

Two bare (unencapsulated) Au-wired cell coupons, C2529-12 and -23, were exposed directly in DH condition to test the cell DH stability, but also to test the reliability of external electrical contact structure and to provide feedback for improving the experimental design. The results showed that a 50~100-h DH exposure readily caused notable to substantial wrinkling and delamination of BZO layer and Al/Ni gridlines over the device areas, along with some blackened regions outside the device areas and corroded spot on the CIGS/Mo layer, as seen in the photographs of Fig. 3. The cell efficiency exhibited a large decrease, regardless of the AZO thickness, from an initial

15~16% to 0%~8% in a fairly random fashion. The loss was mainly due to largely increased series resistance (R_s) and decreased shunt resistance (R_{sh}). Relatively gradual decreases in current density J_{sc} were observed. These are illustrated by normalized I-V parameters for three cells on the bare C2529-12 coupon in Fig. 4. PL and EL imaging also showed largely dimmed light intensity for the cells on both coupons just after 50-h DH exposure (not shown).

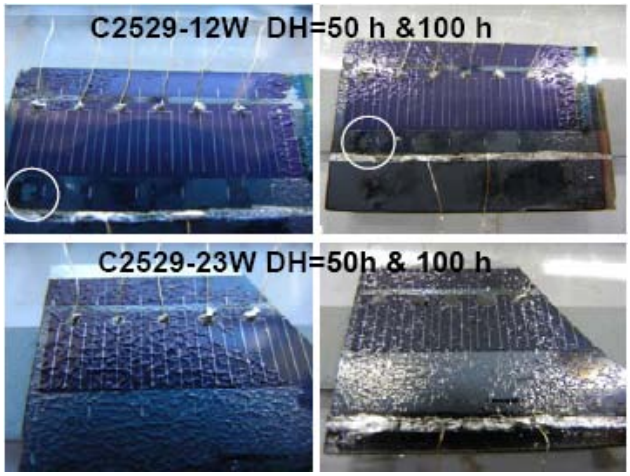

Figure 3 Photographs of two bare cell coupons, C2529-12 with 0.12-µm AZO and C2529-23 with 0.36-µm AZO, exposed in DH for 50 h (left) and 100 h (right). "W" stands for Au wire being soldered. The white circles on C2529-12W indicate the corroded Mo spot.

ECIS measurements indicated that the CIGS solar cells can be represented by a simple equivalent circuit, comprising a series resistance (R_s') for contacts and bulk, and a parallel resistance (R_p) for recombination/diffusion and capacitance (C) for diffusion and depletion [7–9].

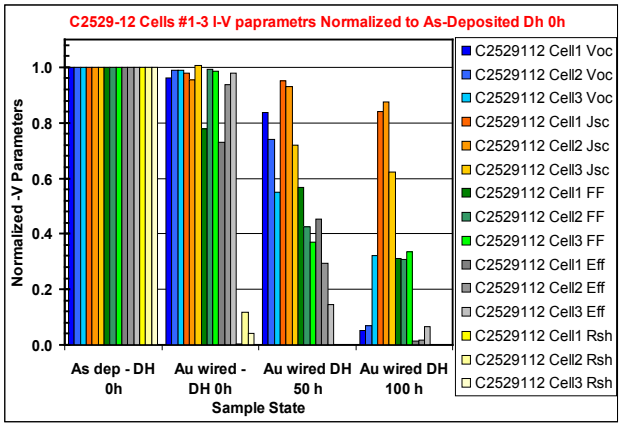

Figure 4 Plot showing changes in I-V parameters normalized to the as-deposited state for three cells on bare C2529-12 coupon with 0.12 µm AZO in four stages: as-deposited, after Au wire soldered, 50-h DH, and 100-h DH exposure.

ECIS curve fitting also confirmed that the solar cells degraded with large increase in R_s', large decrease in the R_p, and some change in C. However, the increase in R_s' was not from the external wiring/soldering, since the DH stability of the Ag paste, solder alloy, and soldered contact with Au wires had been tested to be high in a separate study prior to applying them to the solar cells. To examine whether DH exposure degraded the CIGS solar cells in addition to electrical factors, external quantum efficiency (EQE) measurements were conducted. One of the results is shown in Fig. 5 for C2529-12 cell #1 before and after normalization at 550 nm for 0-, 50-, and 100-h DH exposure. The results suggest that there was certain level of degradation on both CdS-CIGS (400-500 nm range) and AZO (750-1050 nm range).

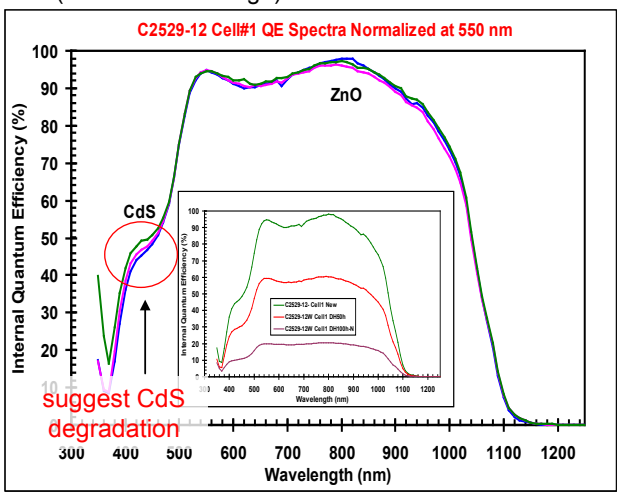

Figure 5 External quantum efficiency (EQE) normalized at 550 nm for C2529-12W cell#1 at 0-, 50-, and 100-h DH exposure. Plots in the inset are for as-obtained EQE, top to bottom: 0, 50, 100 h.

III. DH stability of encapsulated cell coupons

Figure 6 illustrates a borofloat/Al-frame encapsulated sample "Set 5" with four cell coupons inside, which have AZO thickness at 0.12 µm (C2354-4), 0.36 µm (C2354-5), and 0.50 µm (C2354-6 and C2529-13), respectively. Prior to encapsulation of Set 5, the soldered contacts on the cells, In strips on Mo as base contacts, and coupons' edges were coated with epoxy to further ensure the electrical contacts would not degrade by DH. The yellow adhesive Kapton tapes were used to shield the soldered spots for Au wires on tab ribbon pieces from direct exposure to the DH moisture, and were removed before electrical measurements. The >10-mm wide edge sealant tape after lamination was found effective in blocking DH moisture when tested with two "dummy" sets that embedded a $CoCl_2$-based RH indicator strip. The RH indicator strip would change from blue to pink within some hours when TPT was used, but did not change color when a barrier film with WVTR < 10^{-3} g/m^2/day was used. This indicates that TPT would be the primary pathway for DH moisture vapor penetration. Therefore, with a high WVTR

at 142.77 g/m^2/day and breakthrough/equilibrium time at ~3 min/~15 min measured at 86.8^{o}C, the TPT would ensure quick moisture vapor saturation of the ~220-mm^3 chamber space, even only through the small surface area of 1.56-cm^2 from the bottom opening. However, it was also recognized that the edge fringes of the sealant tape inside Set 5 could take up some of the moisture due to its desiccant content of metal oxides. Figure 7 shows the cell efficiency, normalized to that at DH 0h, for the four cell coupons in Set 5 as exposure time increased to 168 h. (A few cells that were poor initially at 0 h were excluded in the plots.)

Upon DH exposure, a major difference observed between the bare and encapsulated CIGS cell coupons was that there was no wrinkling and delamination of any film layer and no Mo corrosion hole on the DH-exposed cell coupons for 168 h. The CIGS/Mo areas outside the cells did show gradual slight blackening on some small areas. This major difference raises a question on whether the degradation mechanisms for direct exposure of bare CIGS cell coupons to the DH moisture vapor are same as for the cells encapsulated, or whether the latter just has a slower rate due to TPT's filtration effect. For the encapsulated test structure, cool-off and dry-out were allowed (typically a few hours to overnight) before I-V and wirings made the measurements convenient.

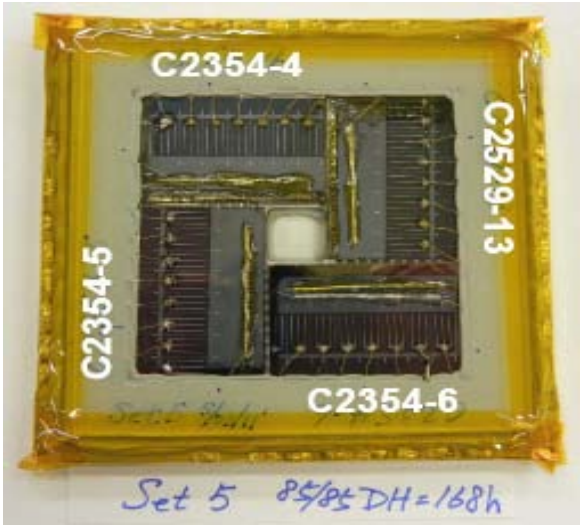

Figure 6 Photograph of sample "Set 5" after 168-h DH exposure. It has four cell coupons encapsulated in the Al frame with a borofloat glass plate on the top and a gray edge-sealant tape around the four sides.

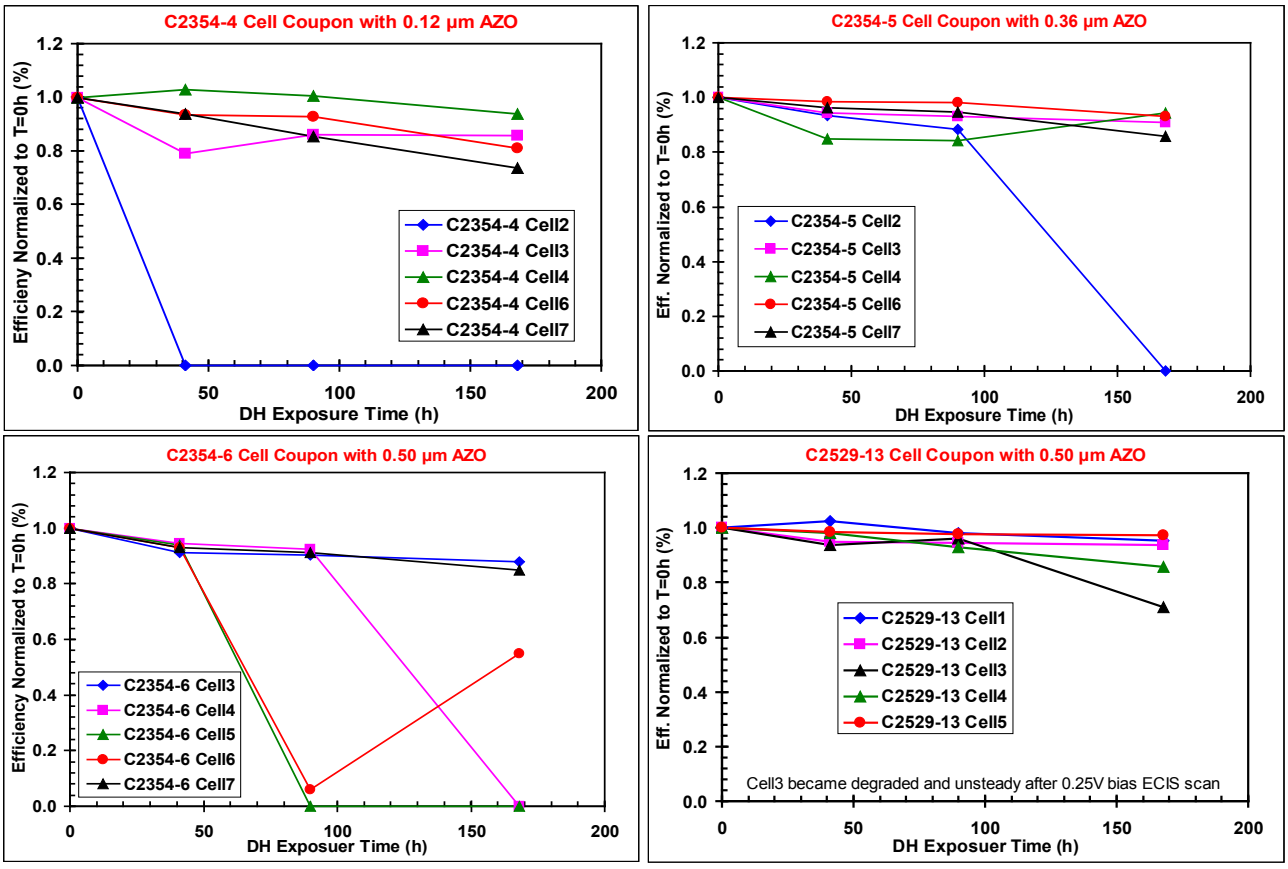

Figure 7 Plots of cell efficiency degradation, as normalized to the efficiency at 0 h, as a function of DH exposure for the four cell coupons in the encapsulated Set 5.

Coupled with epoxy protection, it is quite reasonable to state that the monitored performance degradation of cells in Set 5 is primarily due to cell or materials deterioration, rather than being caused by degradation of the electrical contacts (i.e., Rs from contact points at AlNi pad/Ag paste/solder alloy/Au wire/solder/tab ribbon piece). This assessment was confirmed by the steady R_s' resistance (ECIS measured) with similar contact preparations on AZO or BZO on glass, which was encapsulated and exposed to DH in the same manner but without epoxy coating.

The (normalized) efficiency degradation plots for the multiple cells on the four cell coupons in Fig. 7 show that, except for the C2529-13 coupon, the other three would have one to three cells failed quickly. Most of the cells exhibited gradual degradation. However, a few cells displayed "improved" cell parameters upon DH exposure; its cause is not clear but likely due to heating (curing) effect on the contact spots. Similar to the bare cell coupons, the changes in J_{sc} were relatively gradual, whereas R_s and R_{sh} changes were significant and contributed to the large decreases in open-circuit voltage (V_{oc}) and fill factor (FF) (figures not shown). Figure 8 shows the EQE spectra for C2354-4 cell #4 before (inset) and after normalizing at 550 nm, showing a transmission increase in the 550–1100 nm range, which suggests a degraded AZO layer. Previous studies have shown that, upon DH exposures, AZO (or BZO) increased its transmission in the infrared/near-infrared regions due to loss in ionized-carrier absorption [1,2,5]. The transmission change (normalized at 550 nm) was also seen on C2354-5 (AZO 0.36 µm) and C2354-6 (AZO 0.50 µm) but with

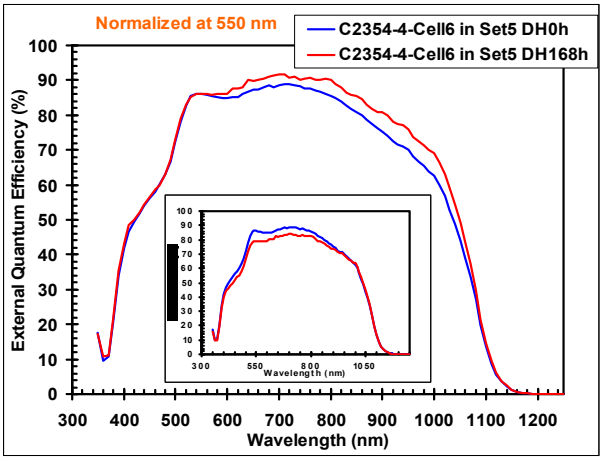

Figure 8 EQE spectra for C2354-4 cell #6 (AZO = 0.12 µm) in Set 5 before and after 168 h DH exposure and normalization at 550 nm.

decreasing extent, as one would expect for thicker AZO from the previous study [1]. Very little change was seen on the least degraded cells on C2529-13 (AZO 0.50 µm). The difference between C2354-6 and C2529-12 (figure not shown) suggests the 0.50-µm AZO layers deposited on separate runs could show some variation.

ECIS results in R_s', R_p and C also reflected the same trend of changes. For example, the semicircle in the complex plane plot for C2354-5 cell #3 became increasingly smaller as DH exposure time increase (not shown). Figure 9 shows a summary plot of R_s', R_p and effective minority-carrier lifetime (or time constant, a product of R_p and C, [8,9]) for C2354-5 cells #3, 5, and 6 obtained from curve fitting of their semicircles with a 0.25 V bias (cells #3 and 5) or none (cell #6). Generally, the trends in R_s' and R_p changes are in parallel to that for the R_s (increased) and R_{sh} (decreased) changes seen in I-V measurements. Capacitance C derived from curve fitting was typically in the range of high 10^{-9} to mid 10^{-8} farads, and decreased as the cell degraded. The lifetime R_p*C for cells #3 and 5 decreased, but increased for cell #6 due to increased R_p, indicating the variation in cell's response to DH-induced stress, which was not revealed from I-V measurements. Work attempting to correlate the ECIS parameters with I-V parameters is underway.

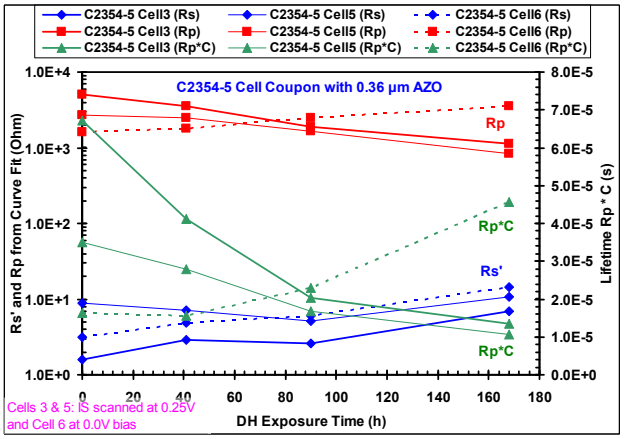

Figure 9 Plots of R_s', R_p, and lifetime (R_p*C) for three cells on C2354-5 (AZO 0.36 µm) as a function of DH exposure time.

By averaging the efficiency only for the gradually degrading cells on each of the four coupons (see Fig. 7), Fig. 10 shows the hourly efficiency degradation rate in DH condition at 85°C and 85% RH, along with the standard deviation, as a function of AZO thickness. With the 0.50-µm AZO cells degraded at different rates (C2354-6 vs. C2529-13), but faster than 0.36-µm AZO cells, the results do not exhibit a strong correlation between cell DH stability and AZO thickness. The causes remain to be further investigated, but we suspect that the higher temperature (> 138°C) and longer time (35 passes) for the deposition of 0.50-µm AZO than that for 0.36-µm AZO (>121°C, 25 passes) may have contributed in a yet-to-be-identified manner to the poorer performance DH stability.

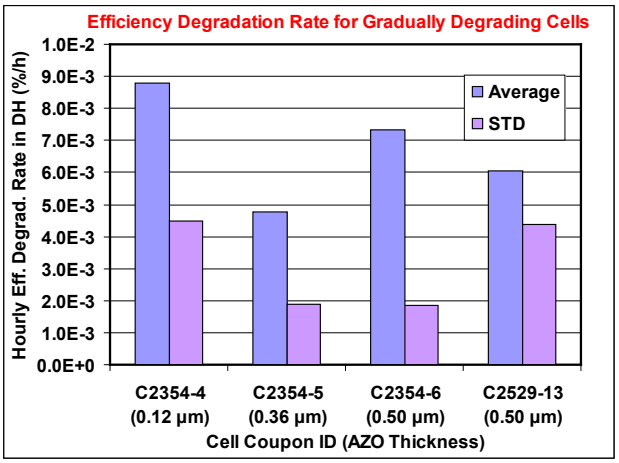

Figure 10 Average hourly efficiency degradation rates (and corresponding standard deviations, STD) for the gradually-degrading cells on the four coupons in Set 5.

CONCLUSIONS

We have investigated the thickness effect of AZO window layer on CIGS cells' DH stability using multiple characterization methods, whereas ECIS, PL, and EL analyses were found complementary to the conventional I-V and QE measurements. The study was facilitated by the use of DH-stable external connections with soldered Au wires for electrical measurements. When exposed directly to DH, bare CIGS cell coupons degraded rapidly in 50–100 h with film wrinkling, delamination, and corrosion of Mo and Ni/Al metal grids, which were not observed on cell coupons encapsulated in a test structure using a TPT backsheet to control moisture ingress. The cell degradation is mainly attributed to series resistance increase, shunt resistance decrease, and AZO degradation. The encapsulated sample continues to undergo DH exposure and shows no wrinkling and delaimation at 270 h. With a limited number of encapsulated cell samples, the current results do not show statistically significant correlation between AZO thickness and cell DH stability as one would expect from the increased DH stability of AZO films on glass substrates. An immediate benefit from the study of bare cells is the replacement of the typical Ni/Al metal grid (0.5/3 µm), which was easily corroded in DH, with DH-stable Ni (>0.2 µm) for newer cell sample sets. More work is underway and the results will be reported in the future.

ACKNOWLEDGEMENTS

The authors thank M. Contreras and T. Gessert for the earlier support of this work and S. Johnston for the support of PL and EL imaging by F. Yan. This work was performed at the National Center for Photovoltaics under DOE Contract No. DE-AC36-08GO28308 with the National Renewable Energy Laboratory.

REFERENCES

[1] F.J. Pern, S.H. Glick, X. Li, C. DeHart, T. Gennett, M. Contreras, and T. Gessert, "Stability of TCO Window Layers for Thin-Film CIGS Solar Cells upon Damp Heat Exposures – Part III," *Proc. SPIE PV Reliability Conference*, 8/2-6/2009, San Diego, CA.

[2] R. Sundaramoorthy, F.J. Pern, C. DeHart, T. Gennett, F.Y. Meng, M. Contreras, and T. Gessert, "Stability of TCO Window Layers for Thin-Film CIGS Solar Cells upon Damp Heat Exposures – Part II," *Proc. SPIE PV Reliability Conference*, 8/2-6/2009, San Diego, CA.

[3] F.J. Pern, B. Egaas, B. To, C.-S. Jiang, J.V. Li, S. Glynn, and C. DeHart, "A Study on the Humidity Susceptibility of Thin-Film CIGS Absorber," *Proc. 34 IEEE PVSC*, 6/7-12/2009, Philadelphia, PA.

[4] R. Sundaramoorthy, F.J. Pern, and T.A. Gessert, "Preliminary Damp-Heat Stability Studies of Thin-Film $CuInGaSe_2$ Solar Cells," *Proc. SPIE PV Conference # 7773 "Reliability of Photovoltaic Cells, Modules, Components, and Systems III,"* 8/1-5/2010, San Diego, CA.

[5] F.J. Pern, S.H. Glick, R. Sundaramoorthy, B. To, X. Li, C. DeHart, S. Glynn, T. Gennett, R. Noufi, and T. Gessert, "Damp-Heat Instability and Mitigation of ZnO-Based Thin Films for $CuInGaSe_2$ Solar Cells," *Proc. 35 IEEE PVSC*, 6/20-25/2010, Honolulu, Hawaii.

[6] M.S. Suresh, "Measurement of Solar Cell Parameters using Impedance Spectroscopy," *Solar Energy Materials and Solar Cells,* **43,** 1996, pp. 21-28.

[7] J. Bisquert, "Theory of the Impedance of Electron Diffusion and Recombination in a Thin Layer," *J. Phys. Chem. B,* **106,** 2002, pp. 325-333.

[8] J. Bisquert, "Impedance Spectroscopy applied on solar cells," a presentation at the Nordic Workshop on Solar Electricity, Sonnerupgaard Gods, Denmark, 27-29 April 2004.

[9] I. Mora-Sero, G. Garcia-Belmonte, P.P. Boix, M.A. Vazquez, and J. Bisquert, "Impedance spectroscopy Characterisation of Highly Efficient Silicon Solar Cells under Different Light Illumination Intensities," *Energy Environ. Sci.*, **2**, 2009, pp. 678–686.

[10] A. Meier, S.H. Glick, and F.J. Pern, "Impedance Spectroscopy as a Non-Invasive Analytical Method for Monitoring Solar Cell Degradation," NCPV Photovoltaics Program Review, *Proc. of 15th Conference*, M. Al-Jassim, J.P. Thornton, and J. M. Gee ed., CP462, Denver, CO, Sept., 1999, pp. 661-666. American Institute of Physics, Woodbury, New York.

[11] H. Bayhan and A.S. Kavasoglu, "Admittance and Impedance Spectroscopy on $Cu(In,Ga)Se_2$ Solar Cells, *Turk J. Phys.* **27,** 2003, pp. 529-535.

[12] H. Bayhan and A.S. Kavasoglu, "Study of $CdS/Cu(In,Ga)Se_2$ Heterojunction Interface Using Admittance and Impedance Spectroscopy," *Solar Energy,* **80,** 2006, pp. 1160-1164.